Influence of bismuth loading in polystyrene-based plastic scintillators for low energy gamma spectroscopy

Guillaume H. V. Bertrand, Fabien Sguerra, Frédérick Carrel, Romain Coulon, Stéphane Normand, Eric Barat, Thomas Dautremer, Thierry Montagu, Matthieu Hamel

Influence of bismuth loading in polystyrene-based plastic scintillators for low energy gamma spectroscopy

G. H. V. Bertrand, F. Sguerra, C. Dehé-Pittance, F. Carrel, R. Coulon, S. Normand, E. Barat, T. Dautremer, T. Montagu and M. Hamel *

CEA, LIST, Laboratoire Capteurs et Architectures Électroniques and Laboratoire Modélisation, Simulation et Systèmes, F-91191 Gif-sur-Yvette, France. E-mail: matthieu.hamel@cea.fr;
Tel: +33 169083325

Abstract

This article presents the synthesis and the blend of bismuth complexes in polystyrene based plastic scintillators. A specific design has enabled the fabrication of a scintillator loaded with up to 17 wt% of bismuth. Tri-carboxylate and triaryl bismuth compounds were used to explore and understand the influence of bismuth loading on the two main criteria of plastic scintillation: light yield and detection efficiency of γ-rays. For gamma radiation with an energy <200 keV, bismuth loaded scintillators demonstrate the ability to produce a photoelectric peak (total absorption peak) in pulse height spectra. The increase of interactions due to bismuth doping was quantified and fitted with standard models. Finally the performance of our bismuth loaded scintillators was evaluated to be better than that of a commercial lead loaded counterpart.

1. Introduction

Radiation detection occupies a central position in nuclear and radiological risk management. Fields such as Homeland Security (facilities control or territorial safety) are in dire need of cheap and high volume radiation detectors. Different technologies can be used but they present major limitations for large scale deployment, for example: High Purity Germanium (HPGe) detectors[1] need a 77 K cooling, and NaI(Tl) scintillators[2] are fragile and expensive to be grown and processed in large volumes.[3] A plastic scintillator has already afforded a set of solutions to this problem as it is cheap, works at room temperature and can be cast or processed into different shapes.[4,5] It is however not the perfect solution for gamma radiation detection,[6] as it only gives scintillation pulses from Compton interactions.[7] These afford spectral information as an edge and it would be interesting to have photoelectric (PE) collision that gives a peak in pulse height spectra. PE peaks are interesting as they are the consequence of total energy absorption from the gamma-ray by the scintillator, therefore allowing their identification. However the PE effect is very unlikely to happen in a plastic matrix because of its weak density and its low effective atomic number (Z_{eff}).[8,9] In order to increase these two parameters, research has been recently focused on the incorporation of heavy atoms in the plastic matrix.[10] The main issue with this approach is the antagonistic effect of the heavy atoms on the scintillation process: heavy metals tend to quench the excited state and decrease the scintillation yields.[11] The challenge of this area is to understand these two effects and find a trade-off between them. For gamma detection the principal focus has been Sn,[12,13] Gd,[14–18] Pb[19–25] and Bi.[26–29] Bismuth has the highest Z among non-radioactive atoms, which makes it a target of choice. Furthermore its derivatives are less toxic than lead or tin equivalents.[30] We can also note that there is no commercially available bismuth loaded plastic scintillator; to the best of our knowledge only lead doped materials are produced.

Knowing that bismuth isotopes have a low neutron cross-section, gamma <200 keV was our primary target in this work, as this range is characteristic of many isotopes of interest such as ^{241}Am or the ^{239}Pu decay chain.

Bismuth chemistry is not very well developed but there are a few known Bi(III) organometallic compounds which are stable, soluble and transparent for our application.[31] $Bi(Ph)_3$ [1] has already been used for this purpose in a poly-(vinylcarbazole) (PVK) matrix.[28] This study gave promising results[29] but the use of PVK poses several limitations as it is very difficult to scale up, very expensive and needs high temperature polymerization that can be incompatible with organometallic stability. The final PVK material is also very fragile as it cannot put up with fast temperature change or mechanical stress. As a response to these challenges we propose here the use of a polystyrene (PS) based plastic scintillator which is cheap and well-known in the literature.[32] We investigated the following postulate correlated with the heavy atom effect: the closer the Bi is to the chromophore the higher the quenching and the lower the scintillation yield will be. We also explored in this study the synthesis and design of new Bi complexes with doped PS matrices for a specific purpose. These Bi-loaded scintillators were shown to give a PE peak for gamma with an energy <200 keV. To complete the understanding of our system we assessed the influence of Bi on the scintillation yield as well as on the PE formation.

2. Results and discussion

From the scarce family of known organo-bismuth compounds stable under light, heat and mild oxidizing conditions, two main families gained our attention, bismuth(III) tri-carboxylates[33] and tri-aryl bismuth(III).[34]

The first family, bismuth(III) tri-carboxylate, was explored at first as it is very close to what have been done by our team with lead loading.[21] Following our previous work with lead di-methacrylate, Bi(III) tri-methacrylate [2] was therefore synthesized using an acid–base pathway from methacrylic acid and $Bi(Ph)_3$ as starting materials (Scheme 1). This reaction presents the advantage of being quantitative and no side products are formed. Other pathways have been tried starting from $Bi(CH_3COO)_3$ or $Bi(NO_3)_3$, but the ligand exchange reaction was not very efficient and isolation was proved to significantly lower the yields. [2] displayed a very good thermal stability, but subsequent experiments showed that its solubility in styrene was limited. For concentration over 8 wt% of [2] in the scintillator, crystals of [2] precipitated at the bottom of the scintillator before there was any evidence of polymerization. Scintillators A1 and A2 containing 3.9 wt% of Bi were tested with a ^{137}Cs source and showed a good response with a very well defined Compton edge (see Fig. S1 in the ESI†). As a consequence we designed different bismuth(III) tri-carboxylates with the perspective of increasing their solubility in styrene. At least one methacrylate was kept on each of our design, as we wanted to keep the heavy metal close to the polymer backbone. We replaced one or two methacrylic substituents with acetic or caproic functions (Scheme 1). The mono- and di-acetate substitution compounds [3] and [4] did not increase the solubility in styrene. But [5] and [6] derivatives bearing longer alkyl chains (respectively mono- and di-caproate compounds) were isolated as very viscous yellowish oils which were totally miscible with styrene. Compounds [5] and [6] can represent up to 45% of the mass of a plastic scintillator when polymerized; thus this kind of polymer achieves remarkably high density (1.39 g cm^{-3}) (Table 1). However [5] and [6] based materials, respectively A3 and A4, were found to have a yellow coloration even at small size, which led to low scintillation yields by self-absorption.[35]

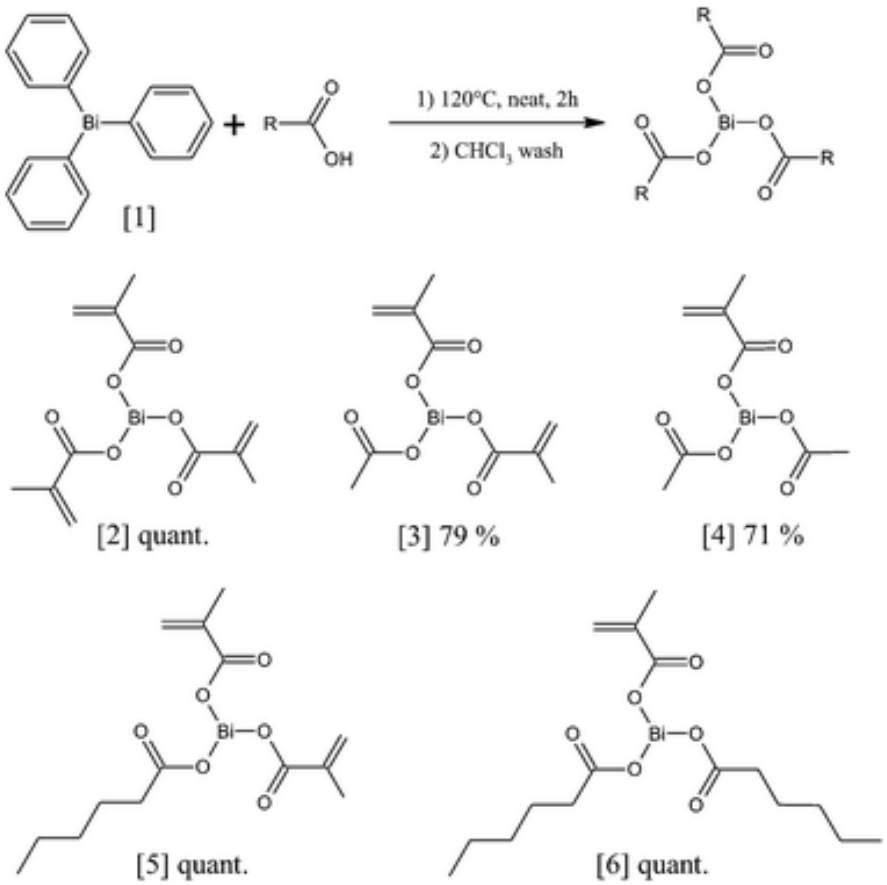

Scheme 1 : Synthesis and yields of different bismuth tricarboxylates

Sample	Bismuth compound	wt% Bi compound	wt% Bi	Density	Light yield [c] (ph per MeV)	Size (cm^3)
A1 [a]	[2]	8	3.9	1.14	2800	2.6
A2 [a]	[2]	8	3.9	1.16	2500	20.8
A3 [b]	[5]	40	17	1.39	600	2.4
A4 [b]	[6]	40	16	1.35	650	2.4

[a] 13 wt% PPO, 0.1 wt% POPOP.
[b] 1.7 wt% PPO, 0.02 wt% bis-MSB.
[c] Relative to EJ-200 in the same geometry.

Table 1 : Properties of bismuth(III) tri-carboxylate based scintillators

The second organo-bismuth stable family we investigated is tri-aryl bismuth(III). Its main representative, $Bi(Ph)_3$ [1], was logically our prime choice for scintillation application following the existing literature.[26–29] But to understand the influence of the Bi localization inside the matrix on the scintillation process it was also decided to synthesize the molecule [7], $Bi(biPh)_3$. For that purpose a synthetic route based on an organo-lithium reagent was used (Scheme 2), providing good isolated yield, and purity was confirmed with the characteristic ^{13}C NMR signal of the C–Bi: 153.8 ppm. The molecule [7] was incorporated in cross-linked polystyrene with suitable chromophores. The resulting scintillator B1 was compared to scintillators B2 and B3 (Table 2). Radioluminescence and pulse height spectra confirm our assumption that linking bismuth covalently to a fluorescent dye dramatically quenches the fluorescence (see Fig. S2 in the ESI).

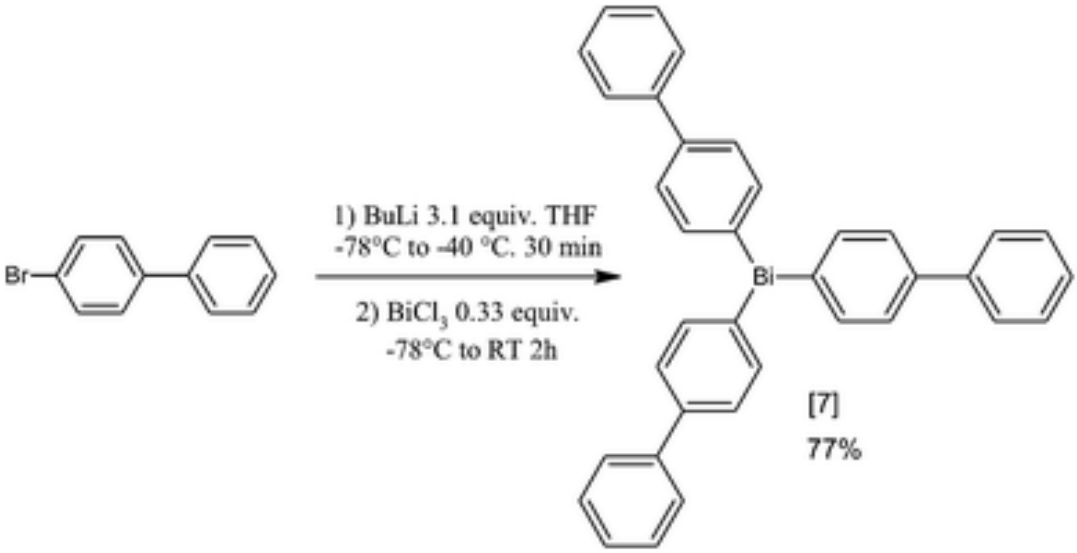

Scheme 2 : Synthesis of tris-(biphenyl)bismuth

Sample	Bismuth compound	wt% Bi compound	wt% Bi	Density	Light yield [b] (ph per MeV)	Size (cm^3)
B1 [a]	[7]	6.2	1.9	1.11	150	7.1
B2 [a]	[1]	4	1.9		975	7.1
B3 [a]	—	—	—	1.09	1350	7.1

[a] 1.9 wt % butyl-PBD 0.1% POPOP.
[b] Relative to EJ-200 in the same geometry.

Table 2 : Properties of triaryl bismuth(III) based scintillators

Another series of scintillators C1 to C6 was synthesized focusing on $Bi(Ph)_3$[1] as our Bi vector to load the polymer matrix. As described in Table 3 the only variable is the Bi loading. The fabrication of these samples followed the classical process for polystyrene based plastic scintillators with the slight difference of the heating temperature. The reaction time (15 days) for this series is then longer than the standard polystyrene process but affords samples with very good optical properties and high density. The sample size was set to 14.7 ± 0.2 cm^3, which is significantly bigger than the majority of Bi-loaded published scintillators. This size choice is justified by the application, gamma ray spectroscopy, and brings us closer to the scales of potential uses (Fig. 1).

Sample	Bismuth compound	wt% Bi compound	wt% Bi	Density	Light yield [b] (ph per MeV)	Size (cm^3)
C1 [a]	—	—	—	1.11	9900	14.7
C2 [a]	[1]	3.7	1.8	1.13	7100	14.7
C3 [a]	[1]	7.1	3.4	1.14	4600	14.7
C4 [a]	[1]	13.3	6.3	1.19	3000	14.7
C5 [a]	[1]	18.7	8.9	1.20	2000	14.7
C6 [a]	[1]	23.5	11.2	1.23	1000	14.7

[a] Matrix given in the experimental part.
[b] Relative to EJ-200 in the same geometry.

Table 3 : Influence of $Bi(Ph)_3$ loading on scintillator properties

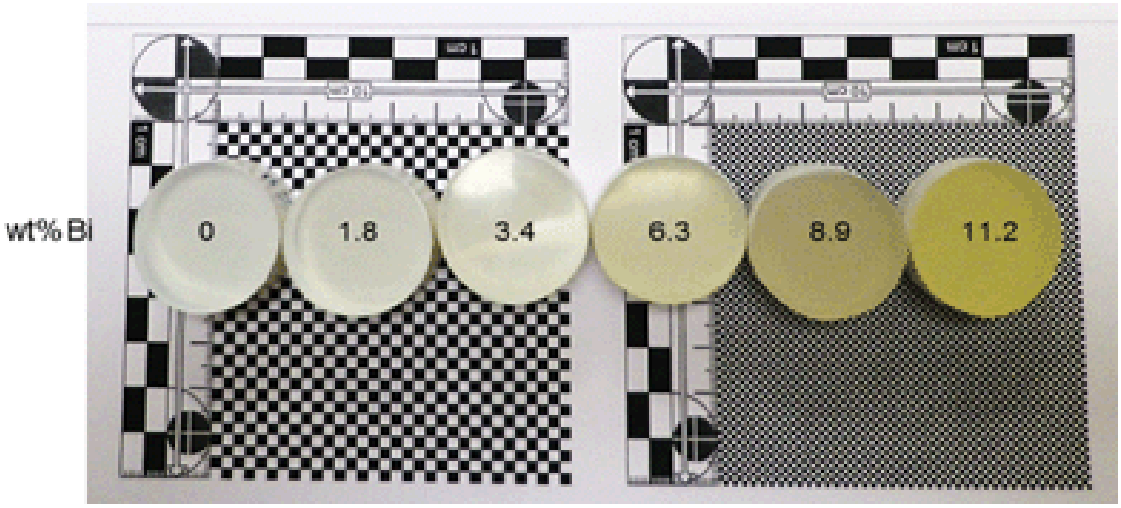

Figure 1 : Plastic scintillators C1 to C6, from left to right, with bismuth loading indicated

The bismuth doping gradient from C1 to C6 was confirmed by an X-ray radiography snapshot (Fig. 2). This experiment also showed the good homogeneity of the samples. The radioluminescence with beta (^{90}Sr/^{90}Y, 25 MBq) (Fig. 3a) and gamma sources (^{137}Cs 206 kBq) (Fig. 3b) was measured to evaluate the impact of bismuth loading on the scintillation yields. We calibrated our measurement with an EJ-200 sample identical in shape, which was set at 10 000 ph per MeV, according to the literature.[36] As expected, the more bismuth we have inside a scintillator the lower is the scintillation yield. The non-linearity of this trend, in the range of bismuth loading presented here, conforms to the prediction by classical models.[37] This was also confirmed by pulse height spectra experiments where **C1** to **C6** were exposed to a 662 keV gamma source (^{137}Cs, 206 kBq), and the Compton edge shift followed the same nonlinear decrease (Fig. 4).

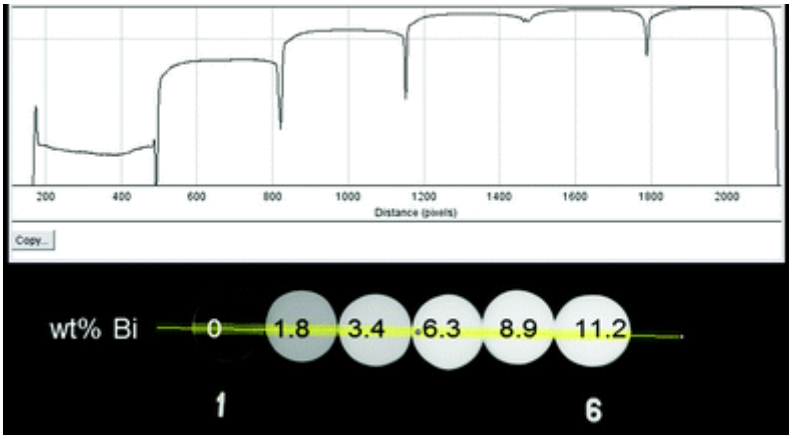

Figure 2 : X-ray radiography snapshot of C1 to C6, from left to right, with bismuth loading indicated. X-ray attenuation profile along the yellow line

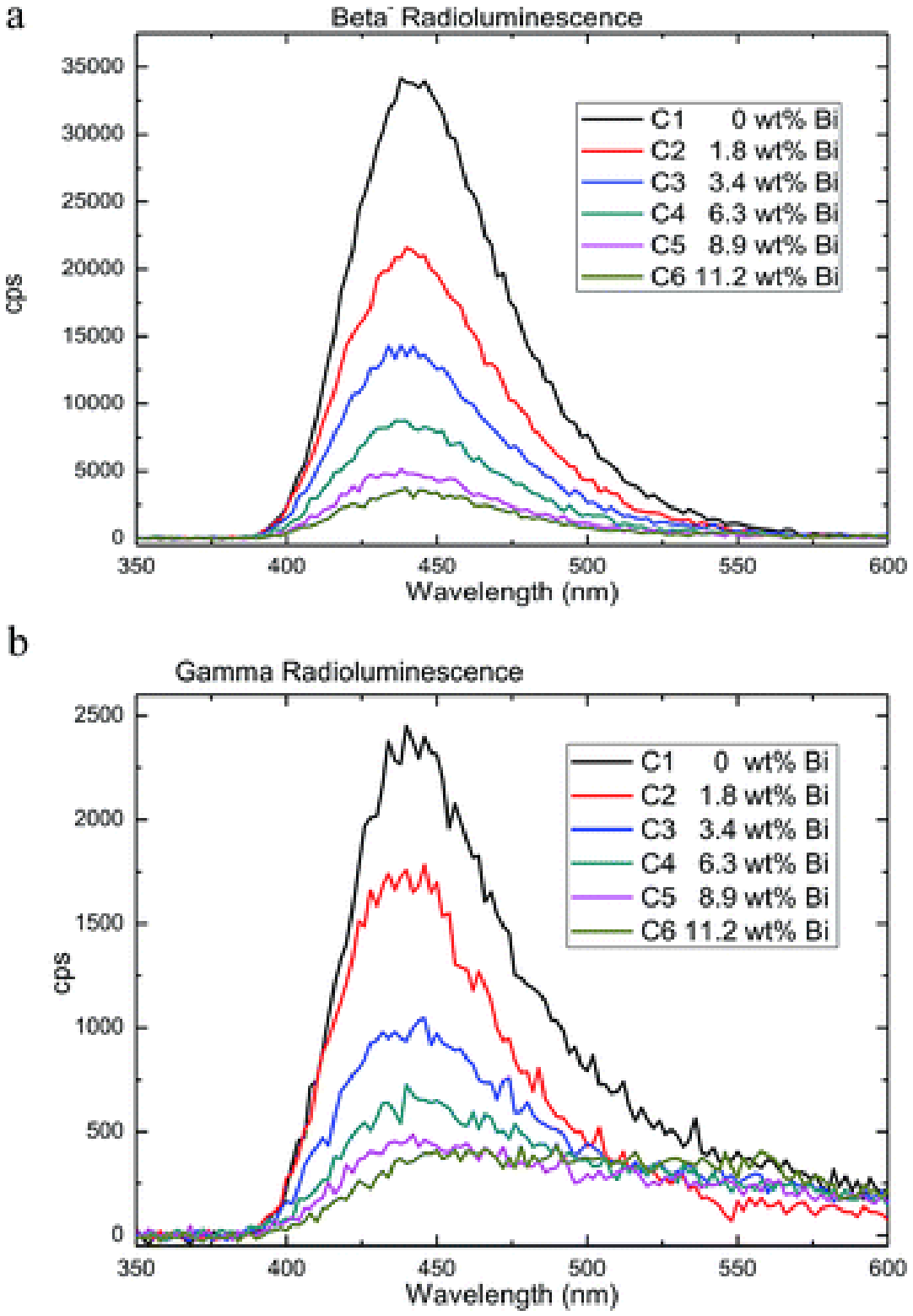

Figure 3 : Radioluminescence experiment on bismuth loaded plastic scintillators with (top) $^{90}Sr/^{90}Y$ (25 MBq) beta source and (bottom) ^{137}Cs (206 kBq) gamma source

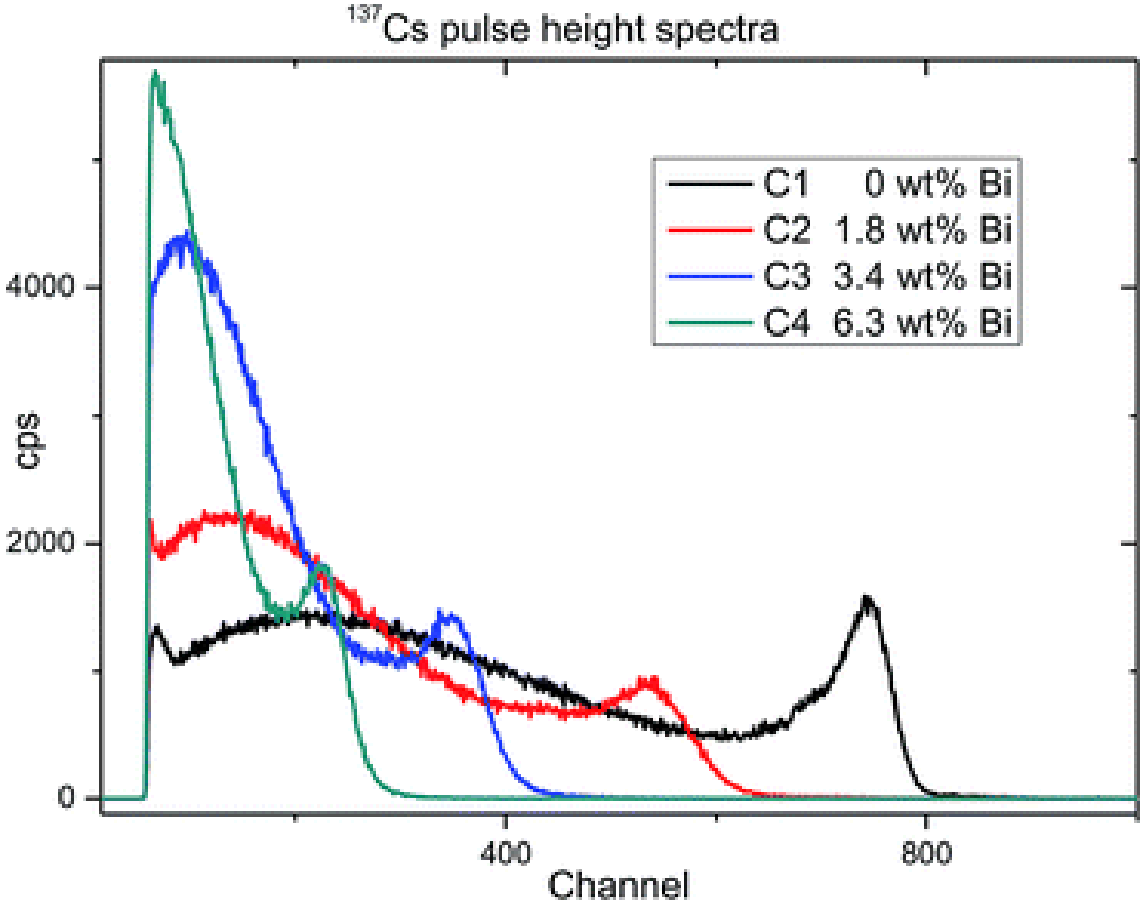

Figure 4 : Pulse height spectra of Bi loaded plastic scintillators

The previous tendencies of scintillation yield evolution versus bismuth loading are condensed in Fig. 5. It showed two significant differences between (1) the beta and gamma experiments and (2) the gamma radioluminescence and pulse height spectra experiments. We explain the first one with consideration of the nature of the ionizing radiation. The beta electron loses its kinetic energy continuously as it enters any scintillator of this size. So the bismuth loading does not affect the interaction's rate; it would only affect the light yield due to fluorescence quenching. A recoil electron from gamma ray loses its kinetic energy continuously from the probabilistic interaction point into the scintillator. However bismuth loading does influence the rate of gamma ray interactions, and artificially offsets the loss of light yield due to fluorescence quenching as the radioluminescence experiment records a flux of photons. The second difference is also linked to this last fact; radioluminescence recorded the sum of the events whereas pulse height spectra sorted each event, separating the counting rate information from the intensity of each event. Hence it is shown here that the influence of bismuth is only on the fluorescence extinction, which experimentally translates to a trend identical to the beta radioluminescence experiment.

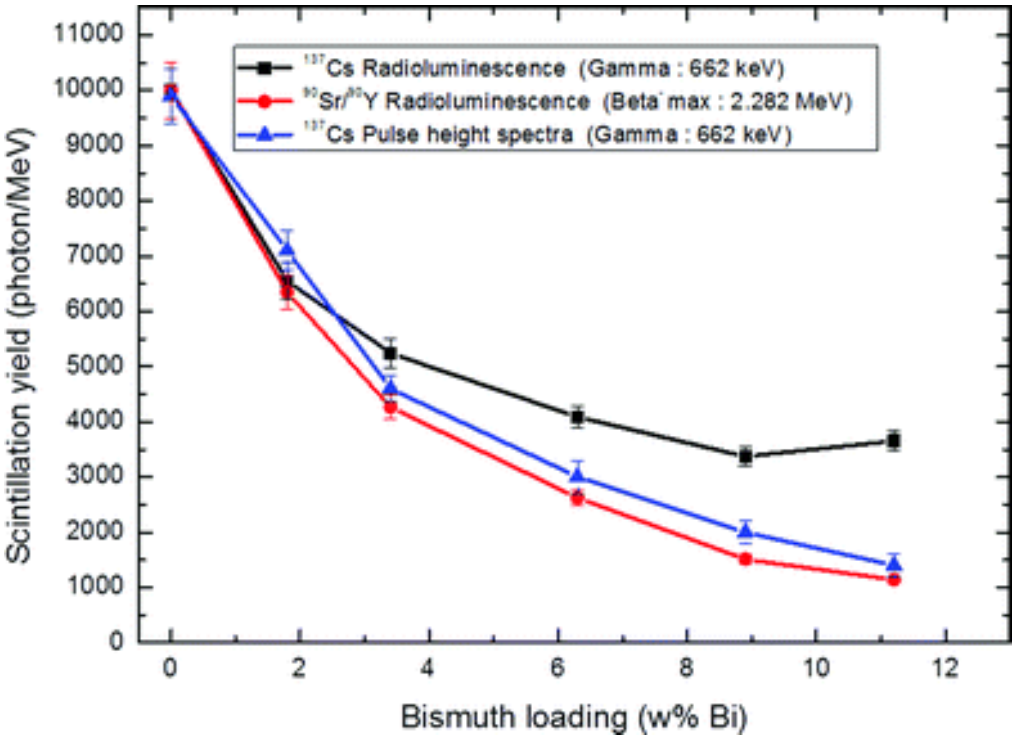

Figure 5 : Evolution of the scintillation yields versus bismuth loading given by gamma (black), beta-(red) radioluminescence, and pulse height spectra of ^{137}Cs (blue)

Unlike no photoelectric peak being observed for C2 to C6 with a ^{137}Cs source, a clear increase of the count rate was noticed as the bismuth loading increased (Fig. 4). Under our experimental setup, a large scintillator doped with Bi accounting for up to 11% of the total mass did not seem to be able to capture all the energy of a 662 keV gamma-ray and to produce PE peaks. To increase the probability of such an event, scintillators C1 to C6 were tested with two lower energy gamma-ray sources: ^{57}Co (122 keV, 0.9 kBq) and ^{241}Am (59 keV, 20 kBq). These measurements were carried out with two different electronic setups (see Experimental), one measuring pulse-height spectra and the other measuring pulse area spectra. This redundancy enabled us to be sure that our observation was not due to any experimental artifact. For both sources the series behaved as expected, showing the apparition of a PE peak and its increase following bismuth loading (Fig. 6). In detail, the ^{57}Co experiments showed the same decrease in scintillation yield, as observed for the ^{137}Cs experiment, and the PE peak apparition and increase. The count rate was calculated by integration, counting the number of PE and, if possible, Compton events. The resulting dataset (Fig. 6a) put in display a clear increase of the count rate from C1 to C5 but not for C6. Hence too much bismuth doping is noxious for our application as it does not give clear compensation to the loss of scintillation yield. The same type of behavior was observed for the ^{241}Am experiment on C1 to C4. Only PE peaks were integrated (Fig. 6b) as the Compton edge was observable only for C1 and C2, as the too low light yield makes Compton pulses fall into the thermoionic and electronic noises. Here again, an optimum value can be defined for the advantages of bismuth loading (PE peak, high count rate) which is antagonized by the scintillation yield's drop. For the observation of the X-ray escape peak, standard simulation (see in the ESI†) showed that it is contained in the Compton edge for ^{57}Co and ^{241}Am, which explains why it was not clearly observed. Simulations were performed to fit the experimental evolution of the counting rate versus the bismuth loading (Fig. 6c and d).

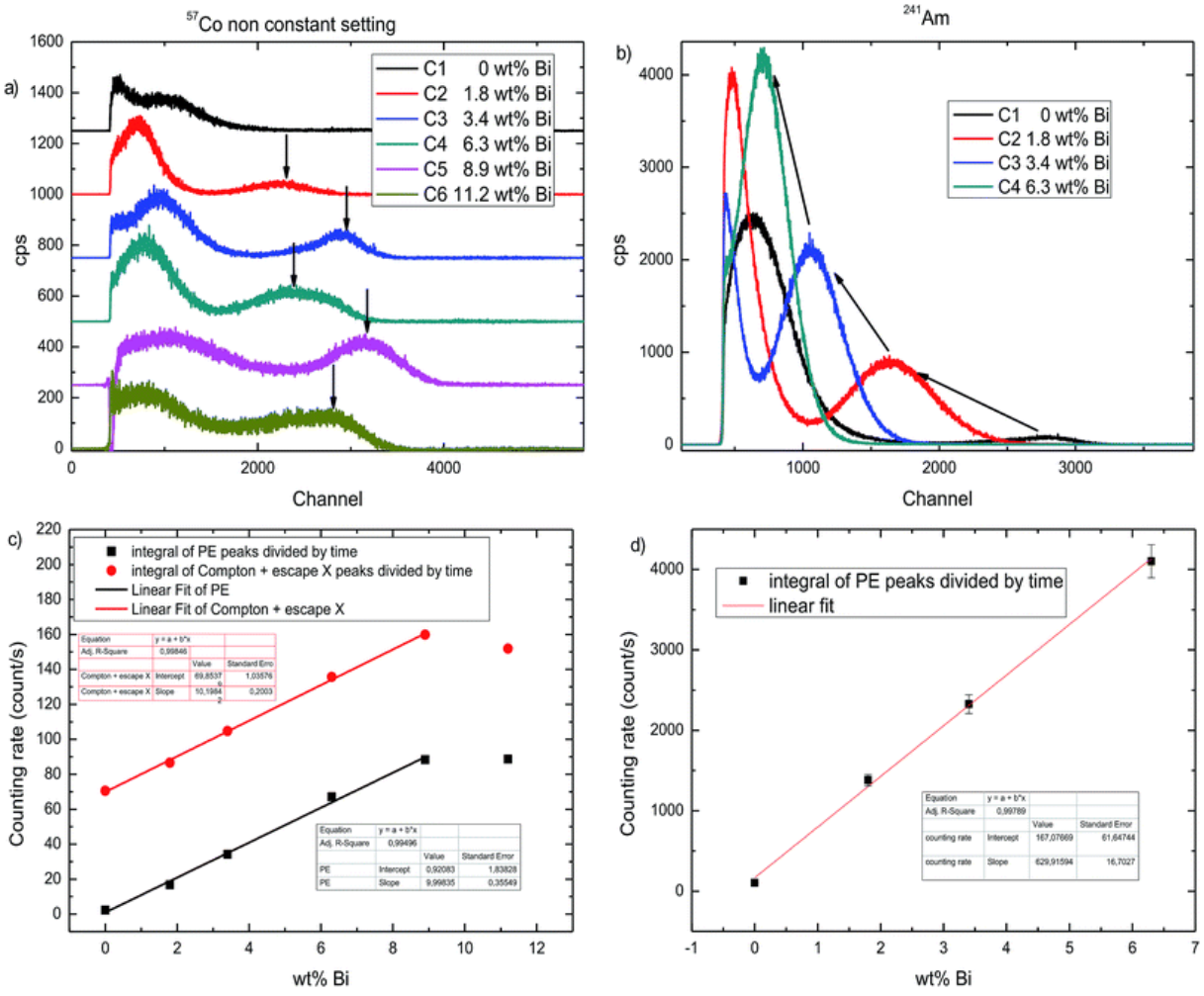

Figure 6 :
(a) Pulse height spectra response of **C1** to **C6** for a ^{57}Co gamma source (primary emission at 122 keV), black arrow indicating the PE peak
(b) pulse height spectra response of **C1** to **C4** for a ^{241}Am gamma source (59 keV)
(c) counting rate versus bismuth loading for events associated with a PE effect (black) and events associated with Compton or escaped X-ray (red) from a ^{57}Co gamma source
(d) counting rate versus bismuth loading for events associated with a PE effect (black) ^{241}Am gamma source

These values were confirmed by digital integration (pulse area experiment) performed with a Lecroy™ digital oscilloscope directly plugged on to the photomultiplier anode. This very simple setup allowed us to observe a photoelectric peak in 10 to 20 seconds depending on the bismuth loading, for a ^{241}Am 20 kBq isotropic source contacting the sample (Fig. 7). Obtaining significant statistics for photoelectric peak identification in such a short time with a plastic scintillator demonstrates the applicative potential of our approach. On the same note we compared our system to two commercially available lead-loaded scintillators (Fig. 8). As expected from the size difference our scintillators gave better light yield than the bigger EJ-256-2%. But counting rates are in the same range (Table 4), which is a promising sign, for our sample is seven times smaller. This is another validation that bismuth loaded styrene based scintillators are competitive with the commercial standards.

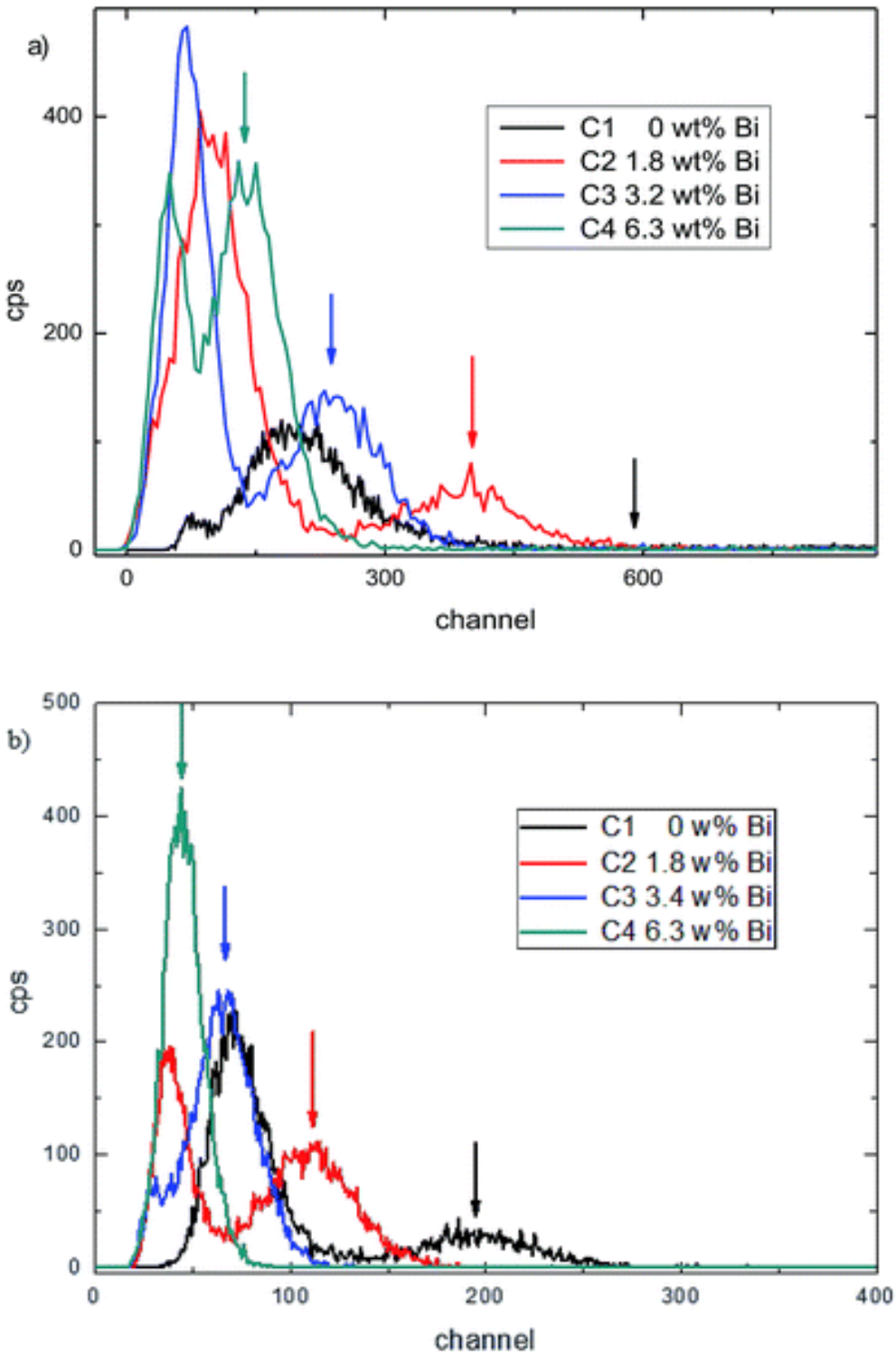

Figure 7 : Pulse area spectra of C1 to C4:
(a) ^{57}Co gamma source (0.9 kBq) – each spectrum was recorded in 180 to 300 s and integrated for 10 000 counts
(b) ^{241}Am gamma source (20 kBq) – each spectrum was recorded in 10 to 20 s and integrated for 10 000 counts

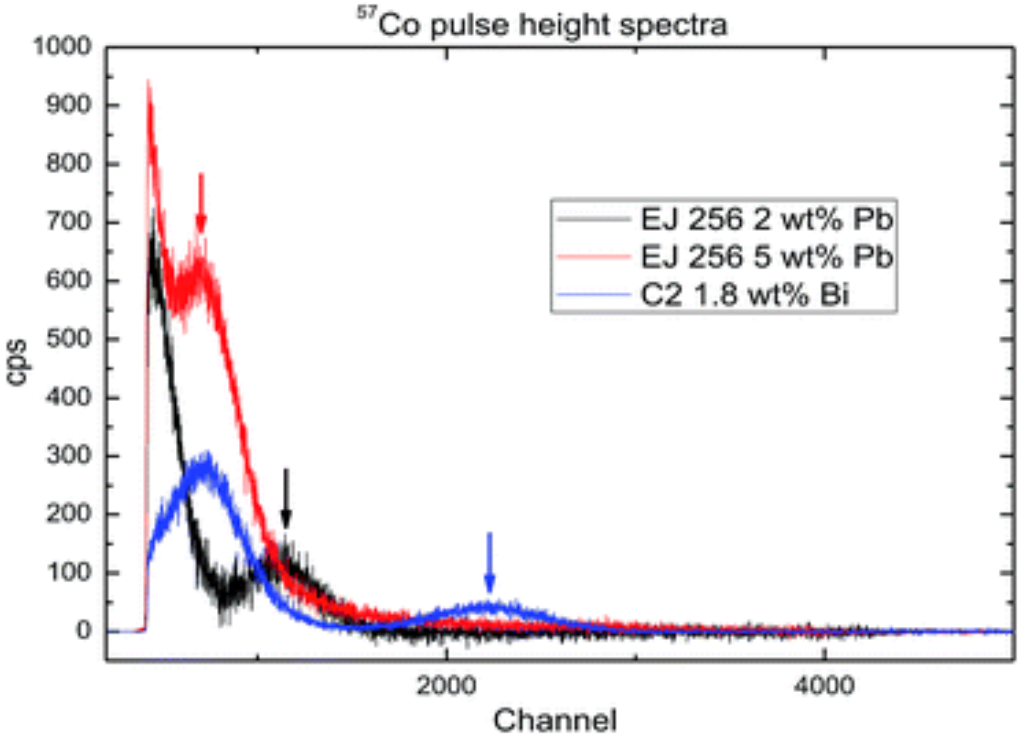

Figure 8 : Comparison between commercial lead loaded plastic scintillators and bismuth loaded plastic scintillator C2 presented in this study

Sample	Loading	Volume (cm^3)	Surface (cm^2)	Light yield (ph per MeV)	^{57}Co PE count rate [b] (counts per s)
EJ-256 (5%)	Pb 5 wt%	98.1	19.6	7200 [a]	200
EJ-256 (2%)	Pb 2 wt%	98.1	19.6	5100 [a]	30
C2	Bi 1.8 wt%	14.7	7.1	7100	17
C3	Bi 3.4 wt%	14.7	7.1	4600	34
C4	Bi 6.3 wt%	14.7	7.1	3000	67

[a] Data from Scionix™.
[b] Semi-Gaussian of the PE peak integrated twice, divided by the measurement duration.

Table 4 : Comparison between lead-loaded and bismuth-loaded scintillators

3. Experimental

3.1.Materials and methods

Solvents were purchased from VWR; reagents were purchased from Sigma-Aldrich except triphenyl bismuth which was acquired from PHDS. Monomers were distilled over CaH_2 under reduced pressure to eliminate inhibitors and impurities. Other reagents were used without further purification. ^{1}H spectra were recorded at 20 °C at 400 MHz on a Bruker AVANCE 400 spectrometer. Chemical shifts (δ) are given in ppm, referenced to the residual proton resonance of the solvents (7.26 for $CDCl_3$; 2.50 for DMSO-D_6). Coupling constants (J) are given in Hertz (Hz). The terms m, s, d, and t refer to multiplet, singlet, doublet, and triplet, respectively; b means that the signal is broad.

3.2.Synthesis

General procedure for bismuth tricarboxylate synthesis. 1 equivalent (2 g, 4.54 mmol) of triphenylbismuth [1] and 3 equivalents (13.62 mmol) of carboxylic acid(s) were sealed inside a 30 mL glass bottle. The mixture was heated until liquefaction of [1] and then vigorously stirred. The resulting liquid was placed in a 100 °C oven for 2 hours and then cooled down to RT. Benzene and other side products were either washed away with 5 mL of chloroform or evaporated under reduced pressure.

[2] Tri-methacrylate bismuth. The general procedure was followed with 1.15 mL of methacrylic acid (13.62 mmol) giving transparent crystals (m = 2.11 g, quant.). ^{1}H NMR: (400 MHz, DMSO-D_6) δ: 5.89 (s, 1H), 5.49 (s, 1H), 1.81 (s, 3H). $C_{12}H_{15}BiO_6$, calculated: C (31.05%), H (3.26%), Bi (45.02%), O (20.68%); found: C (30. 27%), H (3.08%).

[3] (Acetate)di-(methacrylate) bismuth. The general procedure was followed with 0.77 mL of methacrylic acid (2 equiv., 9.08 mmol) and 0.25 mL of acetic acid (1 equiv., 4.54 mmol) giving transparent crystals (m = 1.7 g, 85%). ^{1}H NMR: (400 MHz, DMSO-D_6) δ: 5.89 (s, 2H), 5.50 (s, 2H), 2.03 (s, 3H), 1.81 (s, 6H). The presence of Bi_2O_3 as an impurity was confirmed by IR (ν: 450 cm^{-1}, sharp, low intensity). The Bi_2O_3 ratio (7.2%) was evaluated by elemental analysis. Revised yield of **[3]**: 79%.

[4] Di-(acetate)(methacrylate) bismuth. The general procedure was followed with 0.38 mL of methacrylic acid (1 equiv., 4.54 mmol) and 0.5 mL of acetic acid (2 equiv., 9.08 mmol) giving transparent crystals (m = 1.5 g, 79%). NMR: ^{1}H (400 MHz, DMSO-D_6) δ: 5.91 (s, 1H), 5.50 (s, 1H), 2.03 (s, 6H), 1.81 (s, 3H). The presence of Bi_2O_3 as an impurity was confirmed by IR (ν: 450 cm^{-1}, sharp, low intensity). The Bi_2O_3 ratio (9.0%) was evaluated by elemental analysis. Revised yield of **[4]**: 71%.

[5] (Caproate)di-(methacrylate) bismuth. The general procedure was followed with 0.77 mL of methacrylic acid (2 equiv., 9.08 mmol) and 0.57 mL of caproic acid (1 equiv., 4.54 mmol) giving a pale yellow viscous oil (m = 2.24 g, quant.). ^{1}H NMR: (400 MHz, DMSO-D_6) δ: 5.92 (s, 2H), 5.55 (s, 2H), 2.45 (t, J = 7.5 Hz, 2H), 1.84 (s, 6H), 1.70 (tt, J = 7.5, 7.1 Hz, 2H), 1.37–1.32 (m, 2H), 0.90 (t, J = 7.0 Hz, 3H). $C_{14}H_{21}BiO_6$ calculated: C (34.02%), H (4.28%), Bi (42.28%), O (19.42%); found: C (34.20%), H (4.19%).

[6] Di-(caproate) (methacrylate)bismuth. The general procedure was followed with 0.38 mL of methacrylic acid (1 equiv., 4.54 mmol) and 1.13 mL of caproic acid (2 equiv., 9.08 mmol) giving a pale yellow oil (m = 2.37 g, quant.). ^{1}H NMR: (400 MHz, DMSO-D_6) δ: 5.89 (s, 1H), 5.54 (s, 1H), 2.40 (t, J = 7.6 Hz, 4H), 1.82 (s, 6H), 1.65 (tt, J = 7.5, 7.1 Hz, 4H), 1.35–1.29 (m, 8H), 0.89 (t, J = 7.0 Hz, 6H). $C_{16}H_{27}BiO_6$ calculated: C (36.65%), H (5.19%), Bi (39.85%), O (18.31%); found C (36.13%), H (5.30%).

[7] Tris(biphenyl)-bismuth. 2.22 g of 4-bromo-biphenyl (3 equiv., 9.51 mmol) were added in a 100 mL round bottom flask and purged several times with nitrogen/vacuum cycles. 25 mL of dry THF were added and the resulting solution was cooled down to −78 °C and kept under nitrogen. 10 mL of BuLi in hexane (2.0 mol L^{-1}, 6.2 equiv., 19.9 mmol) was added dropwise giving a bright orange color. The mixture was allowed to reach −40 °C and stirred for 30 min. Prior to the next step, the flask was again cooled down to −78 °C. In a separate 100 mL round bottom flask 1 g of $BiCl_3$ was suspended in 25 mL of dry THF under a nitrogen atmosphere. This suspension was added dropwise using a wide cannula to the aryl–lithium mixture. This mixture was stirred for 1 h and then allowed to reach room temperature over another hour. To the resulting dark brown solution, 10 mL of isopropanol were added to

quench eventual unreacted species. Solvents were evaporated under reduced pressure and the remaining yellow solid was solubilized and hot filtered at ≈90 °C in a 1 : 4 methanol/toluene solvent system. The resulting yellow solution was cooled down and stored at −20 °C overnight. Product **[7]** precipitated as a fine white crystalline powder that was filtered out (m = 1.6 g, 77%). ^{1}H NMR: (400 MHz, DMSO-D_6) δ: 7.91 (d, J = 8.0 Hz, 6H), 7.77 (d, J = 8.0 Hz, 6H), 6.63 (d, J = 7.2 Hz, 6H), 7.46 (dd, J = 7.2, 7.6 Hz, 6H), 7.38 (d, J = 7.6 Hz, 3H). ^{13}C NMR: (101 MHz, DMSO-D_6) δ: 153.7 (3C, C–Bi), 141.0 (3C, quat.), 140.6 (3C, quat.), 138.1 (6C, tert.), 129.2 (6C, tert.), 128.8 (6C, tert.), 127.3 (3C, tert.), 127.0 (6C, tert.). $C_{36}H_{27}Bi$ calculated: C (64.67%), H (4.07%), Bi (31.26%); found: C (64.40%), H (3.98%).

3.3.General procedure for plastic scintillator preparation

Desired solids (fluorescent dyes and Bismuth complexes) and monomers were placed in a suitable round bottom flask. The mixture was put under a nitrogen atmosphere and then frozen using liquid nitrogen and multiple freeze–pump–thaw cycles were performed to achieve total degassing. The resulting solution was heated at 40 °C to achieve total solubilization and poured into a cylindrical glass mold containing a small quantity of the initiator. The filed mold was then purged with nitrogen, and sealed and placed into a 40/45 °C oven for 15 to 30 days. When total polymerization was observed the mold was cooled down to room temperature and then shattered to free the plastic piece. The cylindrical samples were shaped, polished and covered with a reflecting paint for the scintillation experiment.

A1. The general procedure was applied with 1.95 mL of monomers (78 wt%), 0.3 g of PPO (13 wt%), 0.2 mg of POPOP (0.1 wt%), and 0.2 g of **[2]** (8 wt%).

A2. The general procedure was applied with 19.5 mL of monomers (78 wt%), 3 g of PPO (13 wt%), 2 mg of POPOP (0.1 wt%), and 2 g of **[2]** (8 wt%).

A3. The general procedure was applied with 3.50 mL of monomers (58 wt%), 95 mg of PPO (1.7 wt%), 0.6 mg of bis-MSB (0.03 wt%), and 2.24 g of **[5]** (40 wt%).

A4. The general procedure was applied with 8.70 mL of monomers (58 wt%), 95 mg of PPO (1.7 wt%), 0.6 mg of bis-MSB (0.1 wt%), and 2.37 g of **[6]** (40 wt%).

B1. The general procedure was applied with 10.6 mL of monomers (94 wt%), 0.67 g of **[7]** (1 mmol, 6.2 wt%), 0.2 g of butyl-PDB (1.8 wt%), and 10 mg of POPOP (0.1 wt%).

B2. The general procedure was applied with 10.6 mL of monomers (90 wt%), 0.44 g of **[1]** (1 mmol, 4.0 wt%), 0.46 g of biphenyl (3 mmol, 4.1 wt%), 0.2 g of butyl-PDB (1.8 wt%), and 10 mg of POPOP (0.1 wt%).

B3. The general procedure was applied with 10.6 mL of monomers (94 wt%), 0.46 g of biphenyl (3 mmol, 4.2 wt%), 0.2 g of Bu-PDB (1.8 wt%), and 10 mg of POPOP (0.1 wt%).

C1. The general procedure was applied with 21.4 mL of monomers (76.8 wt%), 6.0 g of PPO (23.1 wt%), 20 mg of POPOP (0.1 wt%).

C2. The general procedure was applied with 21.4 mL of monomers (74.1 wt%), 6.0 g of PPO (22.2 wt%), 20 mg of POPOP (0.1 wt%), and 1 g of **[1]** (3.7 wt%).

C3. The general procedure was applied with 21.4 mL of monomers (71.5 wt%), 6.0 g of PPO (21.4 wt%), 20 mg of POPOP (0.1 wt%), and 2 g of **[1]** (7.1 wt%).

C4. The general procedure was applied with 21.4 mL of monomers (66.7 wt%), 6.0 g of PPO (20.0 wt%), 20 mg of POPOP (0.1 wt%), and 4 g of **[1]** (13.3 wt%).

C5. The general procedure was applied with 21.4 mL of monomers (62.5 wt%), 6.0 g of PPO (18.8 wt%), 20 mg of POPOP (0.1 wt%), and 6 g of **[1]** (18.7 wt%).

C6. The general procedure was applied with 21.4 mL of monomers (58.8 wt%), 6.0 g of PPO (17.6 wt%), 20 mg of POPOP (0.1 wt%), and 8 g of **[1]** (23.5 wt%).

3.4.Spectroscopy

X-ray radiography was performed with a Yxlon™ Comet MXR-451 apparatus with the tension set at 50 kV, recorded on a Kodak M-type argentic film.

Pulse height spectra were recorded using a Hamamatsu™ H1949-51 photocathode powered by an Ortec™ 556 High Voltage supply. Output signals were shaped and amplified using a Canberra™ 2111 timing filter amp. Maestro© software combined with a DSPEC analyzer were used to record the spectra. Plastic scintillators were placed on the photocathode using Rhodorsil™ RTV141A optical grease. Radioactive sources were placed either on the scintillator or on a suitable stand, and the setup was isolated from light and kept static in an opaque faraday cage.

Pulse area spectra were recorded using a Hamamatsu™ H1949-51 photocathode powered by an Ortec™ 556 High Voltage supply. Output signals was directly recorded and analyzed on a Lecroy™ waverunner 640Zi oscilloscope. Plastic scintillators were placed on the photocathode using Rhodorsil™ RTV141A optical grease. Radioactive sources were placed either on the scintillator or on a suitable stand and the setup was isolated from light and kept static in an opaque faraday cage.

Radioluminescence spectra were recorded by using the following procedure. In the Fluoromax 4P spectrofluorometer, the excitation light was shut down. In the center of the experiment chamber, $^{90}Sr/^{90}Y$ β-emitting source (25 MBq) or ^{137}Cs γ emitting source (206 kBq) was placed 1 cm away from the scintillator, located close to the detection cell. Spectra were recorded with an integration time of 5 s nm^{-1}. Two types of blank spectra were recorded: one with the plastic scintillator without a source and one with the source without a scintillator, in order to establish a base line. Plastic scintillator EJ-200 was purchased from Eljen Technologies and was used as a reference set at 10 000 ph per MeV.

4. Conclusions

New and classical bismuth complexes have been synthesized and incorporated into polystyrene matrices, affording plastic scintillators with up to 17 wt% content of bismuth [A3] and a density as high as 1.23 [C6], which figure among the best ever recorded values for plastic scintillators. The influence of bismuth loading was analyzed in depth with quantification of photoelectric events, fluorescence quenching and interaction's rate. Our system has been able to generate photoelectric peaks for gamma rays with energy <200 keV with a simple setup in a matter of seconds, and proved to have equal or better characteristics

than those of a lead doped commercial equivalent. This study was performed on samples of 14 cm^3; future experiments will take care of the scale up.

Acknowledgements

We thank the French “Direction Générale de l'Armement” and “Secrétariat Général de la Défense et de la Sécurité Nationale” for the grant associated with this project. Bernard Rattoni is acknowledged for the X-ray radiography snapshot.

Notes and references

1. G. F. Knoll, in Radiation detection and measurement, 2000, p. 405.
2. D. C. Stromswold, E. R. Siciliano, J. E. Schweppe, J. H. Ely, B. D. Milbrath, R. T. Kouzes and B. D. Geelhood, IEEE Nucl. Sci. Symp. Conf. Rec., 2003, 2004, 1065–1069.
3. P. M. Bird and P. R. Burch, Phys. Med. Biol., 1958, 2, 217–228.
4. M. G. Schorr and F. L. Torney, Phys. Rev., 1950, 80, 474.
5. F. D. Brooks, Nucl. Instrum. Methods, 1979, 162, 477–505.
6. E. Nardi, Nucl. Instrum. Methods, 1971, 95, 229–232.
7. S. R. Sandler and K. C. Tsou, J. Phys. Chem., 1963, 860, 300–304.
8. S. R. Sandler and K. C. Tsou, Int. J. Appl. Radiat. Isot., 1964, 15, 419–426.
9. K. C. Tsou, IEEE Trans. Nucl. Sci., 1965, 12, 28–33.
10. V. B. Brudanin, V. I. Bregadze, N. A. Gundorin, D. V. Filossofov, O. I. Kochetov, I. B. Nemtchenok, A. A. Smolnikov and S. I. Vasiliev, in Identif. Dark Matter, Proc. Int. Workshop, 3rd, 2001, pp. 626–634.
11. M. Burton and J. L. Kropp, J. Chem. Phys., 1962, 37, 1752–1756.
12. Z. H. Cho and C. M. Tsai, IEEE Trans. Nucl. Sci., 1975, 22, 72–80.
13. G. I. Britvich, V. G. Vasil'chenko, V. G. Lapshin and A. S. Solov'ev, Instrum. Exp. Tech., 2000, 43, 36–39.
14. E. S. Velmozhnaya, A. I. Bedrik, P. N. Zhmurin, V. D. Titskaya, A. F. Adadurov and D. S. Sofronov, Funct. Mater., 2013, 20, 494–499.
15. A. I. Bedrik, E. S. Velmozhnaya, P. N. Zhmurin, A. F. Adadurov, V. N. Lebedev and V. D. Titskaya, Funct. Mater., 2011, 18, 470–474.
16. L. Ovechkina, K. Riley, S. Miller, Z. Bell and V. Nagarkar, Phys. Procedia, 2009, 2, 161–170.
17. W. Cai, Q. Chen, N. Cherepy, A. Dooraghi, D. Kishpaugh, A. Chatziioannou, S. Payne, W. Xiang and Q. Pei, J. Mater. Chem. C, 2013, 1, 1970–1976.
18. Z. W. Bell, G. M. Brown, C. H. Ho and F. V. Sloop, Proc. SPIE, 2002, 4784, 150–163.
19. G. Turk, C. Reverdin, D. Gontier, S. Darbon, C. Dujardin, G. Ledoux, M. Hamel, V. Simic and S. Normand, Rev. Sci. Instrum., 2010, 81, 10E509.
20. M. Hamel, G. Turk, V. Simic, S. Normand, S. Darbon and C. Reverdin, Proceedings of LSC 2010, 2011, 291–296.
21. M. Hamel, G. Turk, A. Rousseau, S. Darbon, C. Reverdin and S. Normand, Nucl. Instrum. Methods Phys. Res., Sect. A, 2011, 660, 57–63.
22. M. Hamel, S. Darbon, S. Normand and G. Turk, PCT Patent Application WO2012/085004, 2012.
23. M. Hamel, S. Normand, G. Turk and S. Darbon, IEEE proceedings of ANIMMA 2011, 2012, pp. 2–6.

24. M. Hamel, G. Turk, S. Darbon and S. Normand, IEEE Trans. Nucl. Sci., 2012, 59, 1268–1272.
25. A. Rousseau, S. Darbon, S. Girard, P. Paillet, J. L. Bourgade, V. Goiffon, P. Magnan, V. Lalucaa, M. Hamel and J. Larour, Proc. SPIE, 2012, 8439, 84391F1–84391F7.
26. B. L. Rupert, N. J. Cherepy, B. W. Sturm, R. D. Sanner, Z. Dai and S. A. Payne, LLNL Proceedings 480151, 2011.
27. J. Fritsch, D. Mansfeld, M. Mehring, R. Wursche, J. Grothe and S. Kaskel, Polymer, 2011, 52, 3263–3268.
28. B. L. Rupert, N. J. Cherepy, B. W. Sturm, R. D. Sanner and S. A. Payne, EPL, 2012, 97, 22002.
29. N. J. Cherepy, R. D. Sanner, T. M. Tillotson, S. A. Payne, P. R. Beck, S. Hunter, S. Member, L. Ahle and P. A. Thelin, IEEE Nucl. Sci. Symp. Med. Imaging Conf. Rec., 2012, 1972–1973.
30. T. Klapötke, Biol. Met., 1988, 1, 69–76.
31. J. Luan, L. Zhang and Z. Hu, Molecules, 2011, 16, 4191–4230.
32. I. G. Britvich, V. G. Vasil'chenko, V. N. Kirichenko, S. I. Kuptsov, V. G. Lapshin, A. P. Soldatov, A. S. Solov'ev, V. I. Rykalin, S. K. Chernichenko and I. V. Shein, Instrum. Exp. Tech., 2002, 45, 644–654.
33. V. Stavila, J. H. Thurston and K. H. Whitmire, Inorg. Chem., 2009, 48, 6945–6951.
34. D. H. R. Barton, N. Y. Bhatnagar, J.-P. Finet and W. B. Motherwell, Tetrahedron, 1986, 42, 3111–3122.
35. G. F. Knoll, in Radiation detection and measurement, 2000, p. 220.
36. http://www.eljentechnology.com/index.php/component/content/article/31-general/48-ej-200 .
37. A. Sood, R. A. Forster, B. J. Adams and M. C. White, Nucl. Instrum. Methods Phys. Res., Sect. B, 2004, 213, 167–171